

Finite element analysis of coupled phenomena in electromechanical transducers with magnetorheological fluid

Abstract — The paper presents a model of coupled electromagnetic, hydrodynamic, thermodynamic, and mechanical motion phenomena in axial symmetry electromechanical devices with magnetorheological fluid (MRF). The numerical implementation of this model is based on the finite element method and a step-by-step algorithm. The nonlinearity of the magnetic circuit, rheological properties of MRF, and the influence of temperature on properties of the materials have been taken into account. To solve obtained numerical model of phenomena, the iterative Newton-Raphson procedure combined with the block over relaxation method have been applied. The elaborated algorithm has been successfully used to the analysis of the coupled phenomena in MRF brake and clutch.

I. INTRODUCTION

The demand for electromechanical devices with improved functional parameters both in their steady and transient state has been growing in recent years. The research on how to improve these parameters has taken several directions. One of them involves the use of magnetorheological fluids changing their physical properties under the influence of magnetic field. Magnetorheological fluids were invented by Jacob Rabinow in the late 1930s [21]. Their characteristic feature is the viscosity change upon the application of magnetic field. A change in viscosity is inseparably connected with a change of yield stress τ_0 in the fluid. The working principle of magnetorheological electromagnetic transducers is based on the fact that viscosity changes when the fluid is exposed to magnetic field. Naturally, the viscosity of the fluid and the stresses developed in it are related to the magnitude of applied magnetic flux density B . The viscosity and the stresses increase with the growth of the field and so does the yield strength counteracting the motion of moveable parts in the transducers. Owing to their properties, magnetorheological fluids are useful for the efficient control of the transmission of torques and forces. They are used, among others, in brakes, clutches, as well as in rotary and linear dampers [7, 16, 17, 25]. Magnetorheological (MR) transducers are studied in many renowned scientific centers throughout the world. The researches focuses on the analysis of the operating states of existing devices and on the methods of improving their functional parameters but altogether new designs are also under constant development [17, 27, 29, 30]. In order to increase the accuracy of the analysis of steady states and transients of electromechanical devices with MRF, the rheological properties of the fluid, the winding resistance, the resistivity of massive conductive elements, and the magnetic properties of materials should be considered as dependent on temperature [3, 4, 9, 10]. This problem is especially important during the analysis and design of magnetorheological brakes, clutches or dampers [15, 22, 24]. During operation, these devices can easily exceed the allowable temperature of the fluid and destroy its structure [6, 21, 29].

The paper proposes a mathematical model of coupled electromagnetic, hydrodynamic, thermal and mechanical motion phenomena that can be applied to simulate steady and

transient states of the axial symmetry electromechanical transducers with MRF. In order to verify an elaborated algorithm to the analysis of these devices, and an elaborated software, several prototypes of brakes and clutches have been designed and tested.

II. PROPERTIES OF MAGNETORHEOLOGICAL FLUIDS

Magnetorheological fluid is a colloidal suspension of magnetically polarized particles, with diameters of 0.5 to 10 μm , in a carrier fluid, mostly synthetic oil with a low evaporation rate or water [6, 7, 17, 29]. A typical MRF contains from 20% to 80% of ferromagnetic particles, by weight. The main feature of the fluid is its dramatic change of viscosity and, consequently, of shear stress upon the application of magnetic field. The relationship between the yield stress τ_0 and the magnetic flux density B for a few selected types of MRF is shown in Fig. 1. The stress changes during the increase and decrease of magnetic flux density occur in microseconds [7, 17, 23]. The fluids based on a synthetic oil retain their properties in the temperature range from -40°C to 130°C , while the fluids based on the water - from -10°C to 70°C . The magnetization characteristics of the fluids are nonlinear – see Fig. 2. Relative magnetic permeability of the fluids is $\mu_r < 10$.

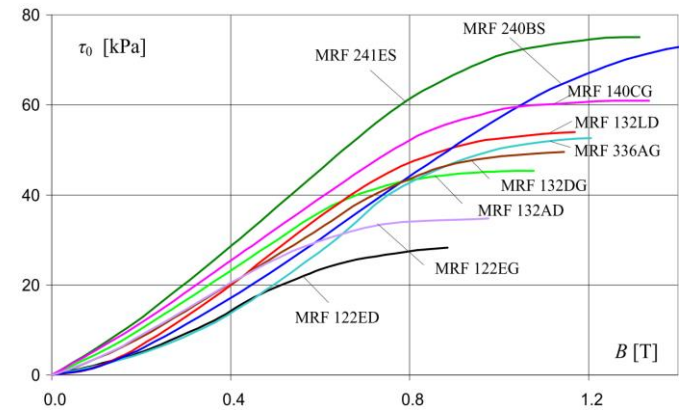


Fig. 1. The characteristics $\tau_0(B)$ of different magnetorheological fluids at 20°C

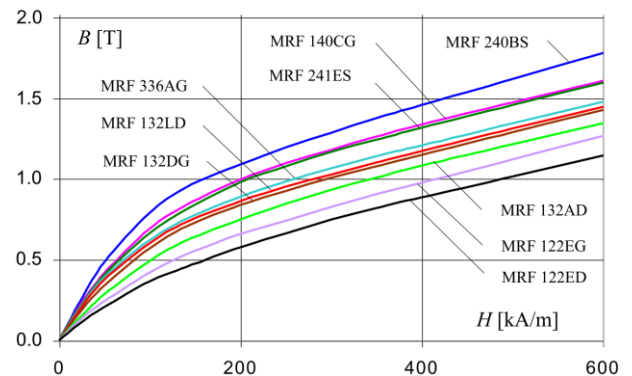


Fig. 2. The characteristics $B(H)$ of magnetorheological fluids at 20°C

III. MAGNETORHEOLOGICAL FLUID APPLICATIONS

Magnetic fluids have a wide range of applications. They are used among others in [1,6,7,15,17,23,27,29,30]:

- brakes and clutches,
- vibration dampers,
- electrically controlled valves with non-moving elements in electro-hydraulic servo-motors,
- packings,
- precise lubrication devices, for example planetary gear transmissions,
- speakers, to dampen the parasitic vibrations of membranes and to enhance the heat transfer from a coil,
- in stepping motors, to damp the rotor oscillation at discrete steps,
- in CD and DVD drives, to reduce head vibrations,
- in state-of-the-art surface polishing devices, as a tool whose shape and hardness can be adapted to the process by changing the strength of a magnetic field,
- medicine, to fight tumours by preventing the blood flow to malignant cells by means of magnetorheological fluids,
- studies and tests of magnetic substances, to establish the size and shape of domains and to detect micro cracks in ferromagnetics.

Below, a short description of the design and properties of magnetorheological brake and clutch built at Poznan University of Technology is presented.

The design of an MR fluid brake is shown in Fig. 3 [23]. The brake is equipped with a cylindrical rotor. The magnetic field is excited by a coil mounted on a stator. The Rheonetic MRF-132LD fluid produced by Lord Corporation has been used in the brake. The diameter and the length of the rotor are 26.8 mm and 27 mm, respectively. The maximum braking torque is ca. 1.7 Nm. One of the advantages of the brake is the low electric power consumption of the winding, not exceeding a couple of watts.

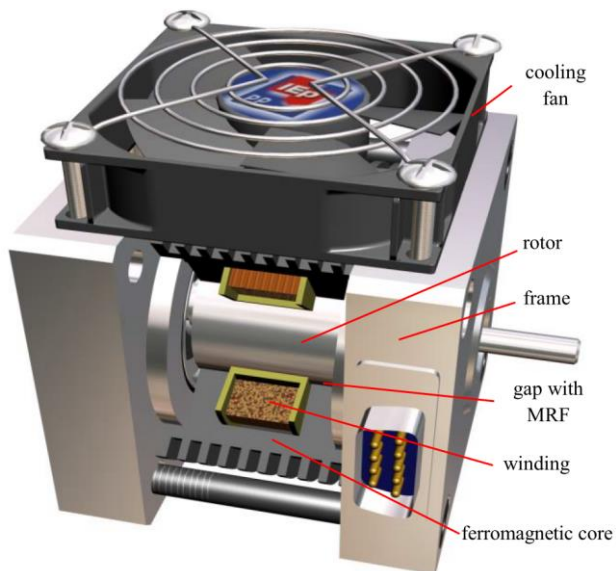


Fig. 3. Magnetorheological brake with electromagnetic excitation

A simplified construction of disk shape MR clutch has been shown in Fig. 4. The analyzed transducer consists of two major components: disk rotor and rotary armature with excitation coil. Between the rotor and the rotary armature there is a gap filled with MR fluid. The fluid type MRF-140CG produced by Lord Corporation has been used in the clutch. The winding that excites magnetic field is located in the rotary armature.

The coil is supplied by slip-rings. The diameter of the rotor is about 140 mm. The prototypes of the considered transducers presented in Figs. 3 and 4 are shown in Fig. 5.

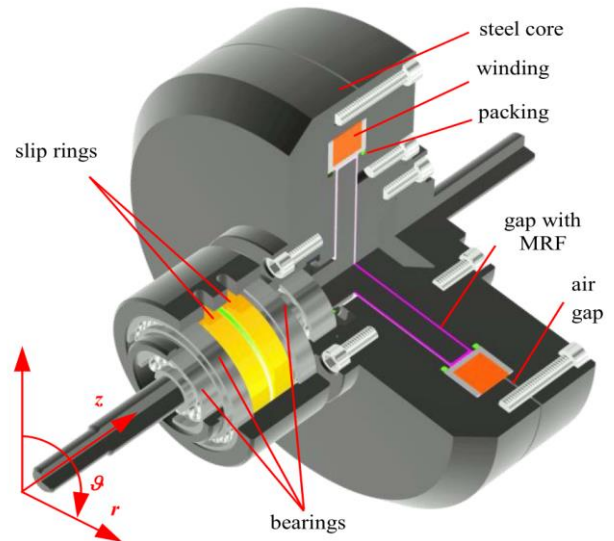


Fig. 4. Magnetorheological disk clutch with electromagnetic excitation

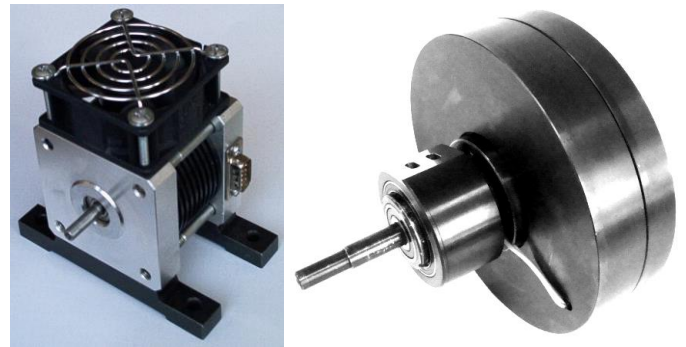


Fig. 5. Prototypes of the elaborated MR brake (on the left) and MR clutch (on the right)

IV. COUPLED PHENOMENA MODEL

The phenomena observed in electromechanical transducers with MRF need to be analysed in terms of fields. In these type of devices, the velocity field of the fluid depends on the angular velocity of the rotor and distribution of the yield stress in the fluid. This stress is function of the magnetic field distribution. The yield strength counteracts the motion of the rotor in the transducer. Therefore, the velocity field of the fluid and the mechanic stress field are coupled with the electromagnetic field. Moreover, the magnetic permeability, the conductivity of the region with eddy currents, the resistances of the windings and the yield stress of the fluid depend on the temperature.

The coupling between fields makes the analysis of the phenomena in a transducer highly complicated. What renders it even more intricate, is the changing character of these fields and the non-linear character of the equations describing them. So far, there are no comprehensive approaches to the problem of solving the time-dependent coupled field phenomena. Most papers in the subject usually deal with the field analysis of some selected phenomena observed in transducers, cf. [2, 12-14, 18, 19].

This paper is an attempt to build a model of coupled phenomena in magnetorheological transducers. The focus is on electromagnetic, hydrodynamic, and thermodynamic phenomena, and on the dynamics of movable elements.

In this paper, the magnetorheological transducers with axial symmetry are considered (see Fig. 3 and Fig. 4). Therefore a cylindrical coordinate system r, z, ϑ is applied. In this case, the equation describing the transient electromagnetic field in a transducer can be expressed as [5,23,24]

$$\frac{\partial}{\partial r} \left(\frac{1}{\mu l} \frac{\partial \varphi}{\partial r} \right) + \frac{\partial}{\partial z} \left(\frac{1}{\mu l} \frac{\partial \varphi}{\partial z} \right) = J - \frac{\gamma}{l} \frac{\partial \varphi}{\partial t} \quad (1)$$

where $l = 2\pi r$, $\varphi = 2\pi r A_\vartheta$, A_ϑ is the component of magnetic vector potential \mathbf{A} in the ϑ -direction, $J = i/s$ is the current density in the winding, i is the winding current, s is the cross-section area of the conductor, μ is the magnetic permeability of the medium, γ is the conductivity of the region with the eddy currents. For the MRF, $\gamma = 0$.

In general, the transient electromagnetic field in MRF devices is voltage-excited. This means that the currents i in the windings are not known in advance, i.e. prior to the electromagnetic field calculation [13,19,25]. Therefore, it is necessary to consider the equations of the electric circuit of the device. The set of independent loop equations may be written as

$$\mathbf{u} = \mathbf{R}\mathbf{i} + \frac{d}{dt} \mathbf{\Psi} \quad (2)$$

where \mathbf{u} is the vector of supply voltages, \mathbf{i} is the vector of loop currents, \mathbf{R} is the matrix of loop resistances, $\mathbf{\Psi}$ is the flux linkage vector. The vector $\mathbf{\Psi}$ is calculated by means of the field model.

The phenomenological approach is used to describe fluid dynamics. In this approach, the fluid is treated as a non-conducting continuum of properties determined by density ρ , dynamic viscosity ν , and magnetic permeability μ [5,20,28]. In the hydrodynamic model, the laminar flow of a non-compressible fluid with no mass sources is investigated [5,28]. It is assumed that the gravitational forces acting on the fluid are negligible comparing to the forces causing its motion in the transducer. The motion of the liquid in the circumferential direction (ϑ direction – see Fig. 4) is caused by the motion of the rotor. For such conditions, the differential equation of the motion of the fluid may be written as [5,14,22]

$$\frac{\partial}{\partial r} \left(\frac{\nu_z}{l} \frac{\partial \phi}{\partial r} \right) + \frac{\partial}{\partial z} \left(\frac{\nu_z}{l} \frac{\partial \phi}{\partial z} \right) = \frac{\rho}{l} \frac{\partial \phi}{\partial t} \quad (3)$$

Here $\phi = 2\pi r v_\vartheta$, where v_ϑ is the component of velocity \mathbf{v} in the ϑ -direction, ρ is the fluid density, and ν_z is the equivalent dynamic viscosity of the fluid.

For the brake, the description of the problem (3) should be completed by nonslip boundary conditions $v_\vartheta = r\omega$ and $v_\vartheta = 0$ on the surface of the rotor and on the frame, respectively, where ω is the angular velocity of the rotor. For the clutch, the boundary conditions for velocity on the surface of the rotor $v_{\vartheta 1} = r\omega_1$ and on the surface of the rotary armature $v_{\vartheta 2} = r\omega_2$ result from mechanical equilibrium equations of clutch moveable elements [15]. In above equations, ω_1 and ω_2 are the angular velocities of the rotor and the rotary armature, respectively.

In the elaborated two-dimensional model of rheological properties of the magnetorheological fluid, the equivalent dynamic viscosity of the fluid is used [23,27]. In order to determine the equivalent dynamic viscosity of the fluid, rheological properties of the fluid are taken into account.

MRFs belong to the non-Newtonian group of fluids. The properties of such fluids can be described by the Bingham model [5,21,18]. A typical characteristic family $\tau = \tau(D, B)$ for a one-dimensional fluid model is presented in Fig. 6, where D is the velocity of deformation [5, 18]. The fluid behaves like a solid body for $|\tau| \leq \tau_0(B)$, and like a body of plastic viscosity η_p for $|\tau| > \tau_0(B)$, $\eta_p = tg(\beta)$.

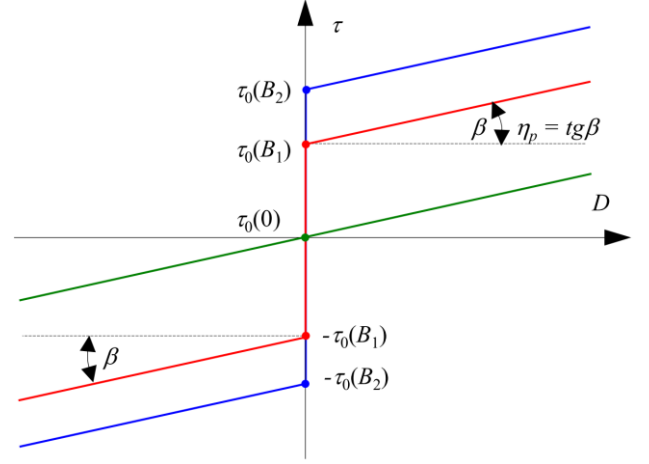


Fig. 6. Typical set of $\tau(D, B)$ characteristics for the MRF

In the elaborated model of a magnetorheological fluid, the equivalent dynamic viscosity of the fluid can be expressed as [15,22]

$$\nu_z = \eta_p + \tau_0(B)/\|\mathbf{D}\| \text{ for } \|\boldsymbol{\tau}\| > \tau_0(B) \quad (4a)$$

$$\nu_z = \infty \text{ for } \|\boldsymbol{\tau}\| \leq \tau_0(B) \quad (4b)$$

The yield stress $\tau_0(B)$ in (4) is determined on the basis of the distribution of the magnetic flux density described by equations (1) and (2). The norms $\|\mathbf{D}\|, \|\boldsymbol{\tau}\|$ of the deformation tensor \mathbf{D} and of the stress tensor $\boldsymbol{\tau}$ [18, 23] can be expressed as

$$\|\mathbf{D}\| = \left(\frac{1}{2} \sum_{i=1}^2 \sum_{j=1}^2 D_{i,j}^2 \right)^{1/2} \quad (5a)$$

$$\|\boldsymbol{\tau}\| = \left(\frac{1}{2} \sum_{i=1}^2 \sum_{j=1}^2 \tau_{i,j}^2 \right)^{1/2} \quad (5b)$$

where

$$D_{i,j} = 0 \text{ for } \|\boldsymbol{\tau}\| \leq \tau_0(B) \quad (5c)$$

$$\mathbf{D} = 0.5 [\nabla \mathbf{v} + (\nabla \mathbf{v})^T] \text{ for } \|\boldsymbol{\tau}\| > \tau_0(B) \quad (5d)$$

$$\tau_{i,j} = (\eta_p + \tau_0(B)/\|\mathbf{D}\|) D_{i,j} \text{ for } \|\boldsymbol{\tau}\| > \tau_0(B) \quad (5e)$$

For one-dimensional fluid model a typical characteristic family $\nu_z(\tau, B)$ is presented in fig. 7.

As mentioned the magnetic permeability μ , the conductivity γ of the region with eddy currents, the resistances of the windings, and the dynamic viscosity ν_z of the fluid are functions of temperature θ . Therefore, the equation describing the distribution of the temperature must be taken into account in the considerations. This equation in the cylindrical coordinates may be written as [5, 20]

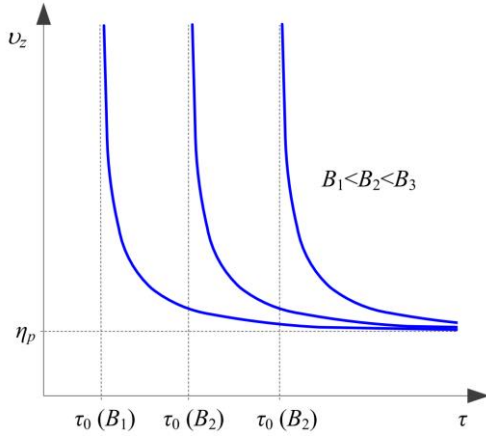


Fig. 7. The relationship between the equivalent viscosity v_z and the stress τ in MRF for $B = \text{const}$

$$\frac{1}{r} \frac{\partial}{\partial r} \left(kr \frac{\partial \theta}{\partial r} \right) + \frac{\partial}{\partial z} \left(k \frac{\partial \theta}{\partial z} \right) = \rho c \frac{\partial \theta}{\partial t} - p \quad (6)$$

where $k = k(\theta)$ is the thermal conductivity, c is the heat capacity.

The quantity p describes the heat source resulting from dissipation of: electrical energy in the conductors, mechanical energy in the viscous fluid, and mechanical energy in the seals and bearings. These heat sources can be expressed as [5, 27]

$$p = \begin{cases} \frac{J^2}{\gamma} & \text{for the winding and the region with eddy currents} \\ v_z \left\{ \left[r \frac{\partial}{\partial r} \left(\frac{v_g}{r} \right) \right]^2 + \left(\frac{\partial v_g}{\partial z} \right)^2 \right\} & \text{for the fluid} \\ \frac{\omega T_s}{V_s} & \text{for the seal} \\ \frac{\omega T_b}{V_b} & \text{for the bearing} \end{cases} \quad (7)$$

where T_s, V_s, T_b, V_b are the friction torques and the volumes of the seal and bearing, respectively.

The description of the problem (6) has been extended by a natural boundary condition on the surface of the frame of the considered MR transducers [20, 23]. It has been assumed that heat flux q_n at the boundary is proportional to the difference of temperatures $(\theta - \theta_a)$ between the surface of the transducer and the surrounding region: $q_n = k \partial \theta / \partial n = -h(\theta - \theta_a)$. In this equation, h is the convection heat transfer coefficient and $\partial / \partial n$ is the derivative in the direction of the outgoing normal to the boundary surface.

When analysing the performance of an MRF electromechanical brake, equations (1), (2), (3), and (6) describing the electromagnetic, hydrodynamic and thermodynamic phenomena must be solved together with the equation of dynamics of its movable elements. For the brake, it assumes the following form

$$J_b \frac{d\omega}{dt} + T_c + T_{fr} = T_{in} \quad (8)$$

where J_b is the moment of inertia of movable elements, $T_c(v_g, B)$ is the braking torque calculated from the yield stress

in the MRF, T_{fr} is the total braking torque produced in the brake by seals and bearings, T_{in} is the driving torque.

For the clutch, the mechanical equilibrium equations can be written as [15]

$$T_{in} - T_c - \text{sgn}(\omega_1) T_{fr} = J_{r1} d\omega_1 / dt \quad (9)$$

$$T_c - \text{sgn}(\omega_2) T_{out} - \text{sgn}(\omega_2) T_{fr} = J_{r2} d\omega_2 / dt \quad (10)$$

where T_{out} is the load torque, ω_1 is the angular velocity of the drive system, ω_2 is the angular velocity of the load system, J_{r1} and J_{r2} are the moments of inertia of the drive and load systems, respectively.

The torque T_c can be determined as an integration of stress tensors along closed surface s placed in the MRF and containing rotor, using the equation

$$T_c = \iint_s r(\tau_g + \tau_{e,g}) ds \quad (11)$$

The vectors $\tau_g, \tau_{e,g}$ in the above equation describe, respectively, the stress in the fluid and the electromagnetic stress acting in the direction g , tangentially to the external surface s of the rotor.

V. FINITE ELEMENT FORMULATION

The equations of presented model of phenomena in MR transducers are coupled through the viscosity function $v_z = v_z(B, v_g)$, the torque $T_c(B, v_g)$, dependence of material properties on temperature, and through the boundary condition $v_g = r\omega$ on the surface of the moving parts. Therefore, these equations should be solved simultaneously. In order to solve non-linear equations (1) – (6) of the coupled phenomena model, only approximate methods can be applied based on the discretization of space and time [11, 27, 31]. The finite element method in connection with Galerkin approach allows to obtain the following system of non-linear differential matrix equations describing the distribution of the magnetic field, currents in the winding, velocity field of the MRF and distribution of the temperature, respectively

$$\begin{bmatrix} S_n + Gp & -w \\ -w^T p & -R \end{bmatrix} \begin{bmatrix} \phi \\ i \end{bmatrix} = \begin{bmatrix} \theta \\ -u \end{bmatrix} \quad (12)$$

$$[S' + G'p] \phi = H \quad (13)$$

$$(S'' + K + G''p) \theta = P + F \quad (14)$$

where S, S', S'' are the magnetic, hydrodynamic, and thermodynamic stiffness matrices, respectively, ϕ, ϕ, θ are the vectors of the nodal values $\phi, v_z,$ and θ , respectively, $p = d/dt$, w^T is the matrix that transforms the potentials ϕ into the flux linkages with the windings, G is the matrix of conductances of elementary rings formed by the mesh, G' is the matrix whose elements depend on the dimensions of the elementary rings and fluid density ρ , G'' is the matrix whose elements depend on the dimensions of the elementary rings and heat capacity c , P is the vector of the nodal heat sources, H is the vector of boundary conditions, K and F are the coefficient matrices describing the heat transport to the surrounding of the transducer [9, 23, 27].

In the considered coupled problems, the elements of windings resistance matrix \mathbf{R} , the elements of conductance matrix \mathbf{G} and reluctance matrix \mathbf{S} in equation (12) depend on the temperature. Thus, $\mathbf{R}=\mathbf{R}(\theta)$, $\mathbf{G}=\mathbf{G}(\theta)$, $\mathbf{S}=\mathbf{S}(\theta)$. When determining the elements of matrices \mathbf{R} and \mathbf{G} , it is assumed that the winding resistance $R(\theta)$ and the conductivity $\gamma(\theta)$ of steel are calculated from the well know equations

$$R(\theta)=R_{20^{\circ}C}[1+\alpha_R(\theta-20)] \quad (15)$$

$$\gamma(\theta)=\frac{\gamma_{20^{\circ}C}}{1+\alpha_\gamma(\theta-20)} \quad (16)$$

where θ is the temperature on the Celsius scale, $R_{20^{\circ}C}$ is the resistance of the winding, $\gamma_{20^{\circ}C}$ is the conductivity of steel at $20^{\circ}C$, respectively, α_R , α_γ are the thermal coefficients of the resistivity of copper and steel, respectively [3, 20].

The elements of the reluctance matrix \mathbf{S} depend also on magnetic permeability of ferromagnetic materials. The magnetic permeability μ is a function of the magnetic field and temperature θ . The permeability can be determined on the basis of the family of $B(H)$ characteristics measured for $\theta = \text{const}$. For the purpose of calculations of μ , these characteristics can be gathered in a table. However in order to minimize the calculation time, it is better to use the analytical dependency $\mu(H, \theta)$ for approximation of the results obtained from measurements. The equations approximating the permeability dependence on temperature and magnetic field H are formulated in such a way that after the material reaches the Curie temperature θ_C , the relative permeability is equal to unity. For this purpose the following expression is used [3, 8]

$$\mu(H, \theta) = \mu_0 \left(1 + \frac{c_1}{1 + \frac{H}{c_2}} \sqrt{\frac{\theta_C - \theta}{\theta_C}} \right) \quad (17)$$

where μ_0 is the magnetic permeability of the vacuum.

Parameters c_1 , c_2 are selected in such a way that the curve described in equation (17) reflects as closely as possible the results of the measurements.

The developed algorithm of the analysis of coupled phenomena in the formulation of equation (14) takes into account the fact that thermal conductivity of materials k depends on temperature. It is assumed that this dependence is shown by the following equation [3, 9, 27]

$$k(\theta) = k_{20^{\circ}C} [1 + \chi(\theta - 20)] \quad (18)$$

where $k_{20^{\circ}C}$ is the thermal conductivity of the material at $20^{\circ}C$, χ is the thermal conductivity temperature coefficient. Temperature also affects the rheological properties of the magnetorheological fluid. This was confirmed by the investigations of fluids MRF 132LD and MRF 132AD performed at the Poznan University of Technology [26, 27]. Exemplary results of the tests of the influence of temperature θ and magnetic flux density B on shear stress for fluid MRF 132LD are shown in Fig. 8. It can be seen that the stress drop is roughly proportional to the increase of the temperature. The influence of temperature θ and velocity of deformation D on the equivalent viscosity ν_z is shown in Fig. 9. This figure

shows that the change in viscosity as a function of temperature, for constant magnetic flux density B and velocity of deformation D , can be approximated by means of the linear function

$$\nu_z(\theta) = \nu_z(\theta_o, B) [1 - a_\nu(\theta - \theta_o)] \quad (19)$$

where a_ν is the temperature coefficient of viscosity changes, $\nu_z(\theta_o, B)$ is the viscosity at a reference temperature θ_o and magnetic flux density B .

Equation (19) is used for the calculation of the elements of matrices \mathbf{S}' and \mathbf{H} in equation (13).

In the elaborated model of coupled phenomena, the effects of temperature on the heat capacity c of materials and the influence of mechanical stress in magnetic materials on magnetic permeability μ have been neglected.

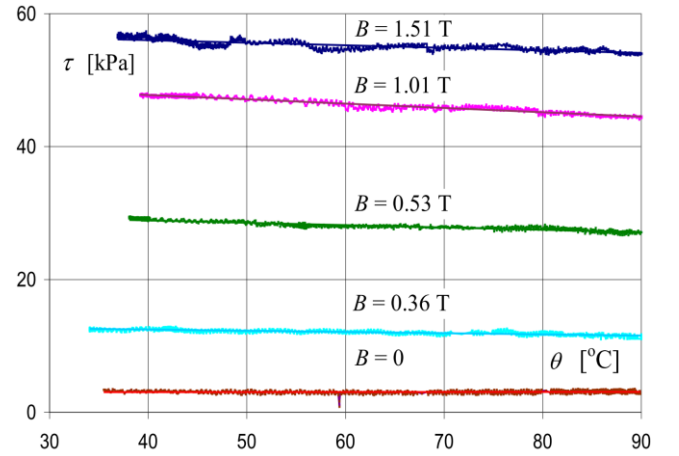


Fig. 8. Family of $\tau(\theta, B)$ characteristics for fluid MRF 132LD at $D = 800 \text{ s}^{-1}$

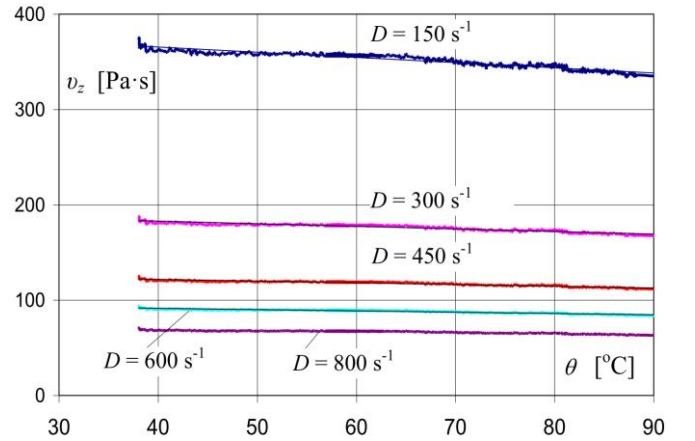


Fig. 9. Family of $\nu_z(\theta, D)$ characteristics for MRF 132LD fluid at $B = 1.51 \text{ T}$

In order to solve the equations of the presented model of coupled electromagnetic, hydrodynamic, thermal and mechanical phenomena in an MR transducer in the time domain the time-stepping method has been applied. The backward difference scheme for the approximation of the time-derivatives in equations (12), (13) and (14) was applied. The time discretization leads to the following system of non-linear algebraic matrix equations

$$\begin{bmatrix} \mathbf{S}_n + \Delta t^{-1} \mathbf{G}_n & -\mathbf{w} \\ -\mathbf{w}^T & -\Delta t \mathbf{R}_n \end{bmatrix} \begin{bmatrix} \boldsymbol{\varphi}_n \\ \mathbf{i}_n \end{bmatrix} = \begin{bmatrix} \Delta t^{-1} \mathbf{G}_n \boldsymbol{\varphi}_{n-1} \\ -\Delta t \mathbf{u}_n - \mathbf{w}^T \boldsymbol{\varphi}_{n-1} \end{bmatrix} \quad (20)$$

$$[S'_n + \Delta t^{-1}G'_n]\phi_n = \Delta t^{-1}G'_n\phi_{n-1} \quad (21)$$

$$[S''_n + K_n + \Delta t^{-1}G''_n]\theta_n = \Delta t^{-1}G''_n\theta_{n-1} + P_n + F_n \quad (22)$$

where n denotes the number of time-steps, Δt is the time-step length.

In order to approximate the time-derivatives in equations (8), (9) and (10) describing the motion of the movable element of the brake and the clutch, an explicit formula has been used [15,22]. For the brake

$$J_b(\alpha_{n+1} - 2\alpha_n + \alpha_{n-1})/(\Delta t)^2 = T_{in,n} - T_{c,n} - T_{fr,n} \quad (23)$$

where α is the angular position of the rotor, $T_{in,n} = T_{in}(t_n)$, $T_{c,n} = T_c(t_n)$, $T_{fr,n} = T_{fr}(t_n)$.

The angular velocity ω of the rotor may be calculated according to the formula

$$\omega(t_n + 0.5\Delta t) = (\alpha_{n+1} - \alpha_n)/\Delta t \quad (24)$$

The braking torque $T_{c,n}$ is described by formula (11). In the considered brake, the component B_θ of the magnetic flux density \mathbf{B} is equal to zero. Therefore, in (11) the component $\tau_{c,\theta}$ of Maxwell stress tensor is equal to zero. Time discretisation of motion equations for the clutch lead to the following relationships [15]

$$\omega_{1,n} = \Delta t \left((T_{in,n} - T_{fr,n} - T_{c,n})/J_{r1} + p\omega_1|_{n-1} \right) / 2 + \omega_{1,n-1} \quad (25)$$

$$\omega_{2,n} = \Delta t \left((T_{c,n} - T_{fr,n} - T_{out,n})/J_{r2} + p\omega_2|_{n-1} \right) / 2 + \omega_{2,n-1} \quad (26)$$

where p is time derivative, $\omega_{1,n} = \omega_1(t_n)$, $\omega_{2,n} = \omega_2(t_n)$, $\omega_{1,n-1} = \omega_1(t_{n-1})$, $\omega_{2,n-1} = \omega_2(t_{n-1})$, $T_{out,n} = T_{out}(t_n)$.

The primary difficulty in obtaining a numerical solution of the magnetorheological fluid flow problem, given by equation (3), is the existence of a surface separating the regions of sheared and non-sheared fluid [3,25]. The position of this surface is not known in advance, i.e. prior to the velocity field calculation [14]. The use of the previously described equivalent dynamic viscosity formulations eliminates the need of tracking the surface separating these two flow regions and simplifies the solution. It leads, however, to singularities since the equivalent dynamic viscosity ν_z attains an infinite value in the regions where $\|\mathbf{D}\|=0$, i.e. in the regions where the fluid behaves like a solid body. In order to avoid such a problem, equations (4.a) and (4.b) are replaced by following equation proposed in [14]

$$\nu_z = \eta_p + \frac{\tau_0}{\|\mathbf{D}\|} (1 - e^{-m\|\mathbf{D}\|}) \quad (27)$$

where m is an exponential growth parameter.

This approach has been utilized to provide a good approximation of the Bingham fluid properties for both low and high shear stresses τ . Extensive numerical experimentation led to the establishment of $m = 100$ as high enough to obtain accurate solutions [14, 23].

Due to the nonlinearity of physical properties and couplings between the considered phenomena, the equations (20) – (26)

should be solved simultaneously. In the elaborated algorithm and computer software, these equations are solved with the aid of the Newton iterative method and the block over relaxation procedure [4,9,27].

VI. RESULTS

The discussed algorithm for solving the equations of coupled phenomena model was implemented in a computer program which allows to simulate coupled phenomena in the magnetorheological transducers with axial symmetry. The program has been developed in the Borland Delphi environment. The program was used for the simulation of the magnetorheological brake and clutch operation. The transients and the steady state in the prototypes of electromagnetic brake and clutch shown in Fig. 3 and Fig. 4, respectively, were considered. It was assumed that the delay values for which the fluid reacts to the changes in the magnetic field are neglected. First, the elaborated program was used to determine the electromagnetic field, the velocity field of the fluid, and the distributions of the temperature when constant voltage is applied to the winding of the brake. The 132LD MRF produced by Lord Corporation was used in the brake. It was assumed that the rotor's angular velocity ω equals 150 rad/s. In the consideration, it was assumed that the magnetic field and the temperature field are calculated using the same mesh. In the region with the magnetorheological fluid, only a part of this mesh was used. The influence of the density of mesh on the results of calculations was analyzed. The density was increased until a difference between two consecutively calculated values of currents or torques were observed. The length of the time step was chosen as equal to 0.00005s. With such time step, the calculations lasted very long. Therefore, in the calculations presented in this paper, in order to reach the steady state, the elements concerning time derivatives were neglected in equations (20) – (22). Selected examples of the distributions of magnetic field lines, the respective distributions of lines connecting the points with identical velocity values, and the distributions of the isothermal lines are shown in Fig. 10.

Next, dynamic states in a brake driven by an induction motor were analysed. The motor was supplied from an inverter. The characteristic $T_{in}(\omega)$ of the motor and the braking torque $T_{fr}(\omega)$ from equation (8) associated with friction were measured. A bench for magnetorheological brake test is shown in Fig. 11. The test bench can be used to measure and register time characteristics-of torque, rotational speed, supply voltage, and current in the excitation winding.

A transient state associated with supplying the field-exciting coil in the brake was considered. It was assumed that prior to the voltage supply, the angular velocity ω of the motor was equal to 50 rad/s. The calculated torque-time $T(t) = J_b d\omega/dt + T_c + T_{fr}$, current-time $i(t)$, and angular velocity-time $\omega(t)$ characteristics are shown in Fig. 12.

In order to verify the calculations, the driving torque $T_{in}(t)$, the current $i(t)$, and the angular velocity $\omega(t)$ were measured on the prototype of the brake. The results are shown in Fig. 13. The investigation proved that for the considered working conditions, the time characteristic of the braking torque is multiexponential.

The steady states of the MRF brake were also investigated. A prototype brake was tested with two MR fluids: MRF 132AD and MRF 132LD. The influences of the properties of MR fluids and the length g of the gap between the stator and the rotor on the parameters of the brake were examined.

Selected measured relationships between the braking torque and the rotational speed of the rotor at a constant exciting current are shown in Fig. 14. It follows from this figure that for both types of MR fluids, the braking torque does not change significantly at rotational speeds exceeding 250 rpm.

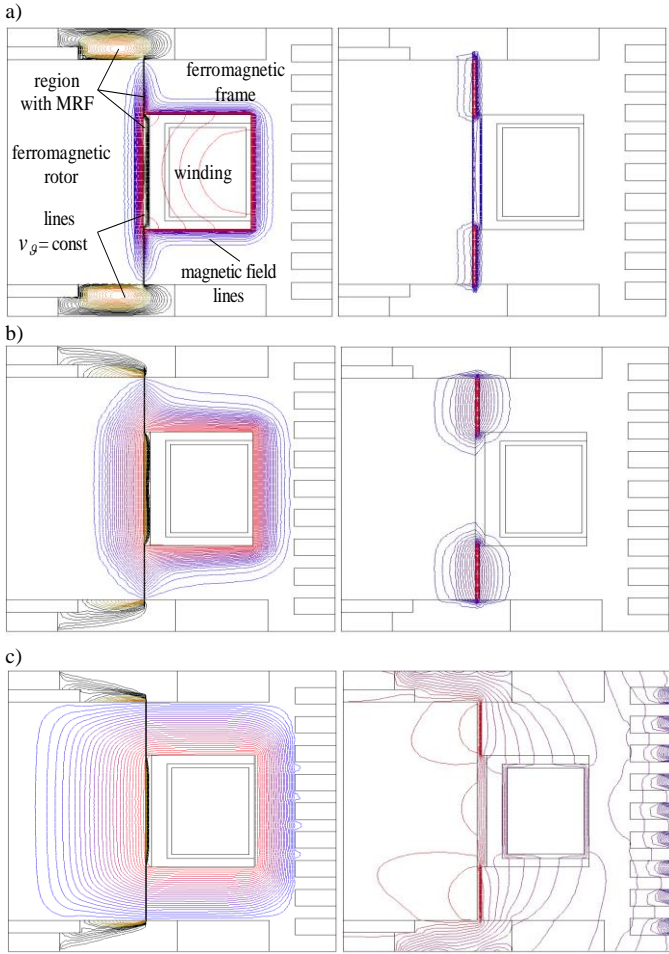


Fig. 10. Distributions of the magnetic field lines, the lines $v_g = \text{const}$ (on the left) and the isothermal lines (on the right) for: a) $t = 0.0001$ s; b) $t = 0.01$ s and c) steady state

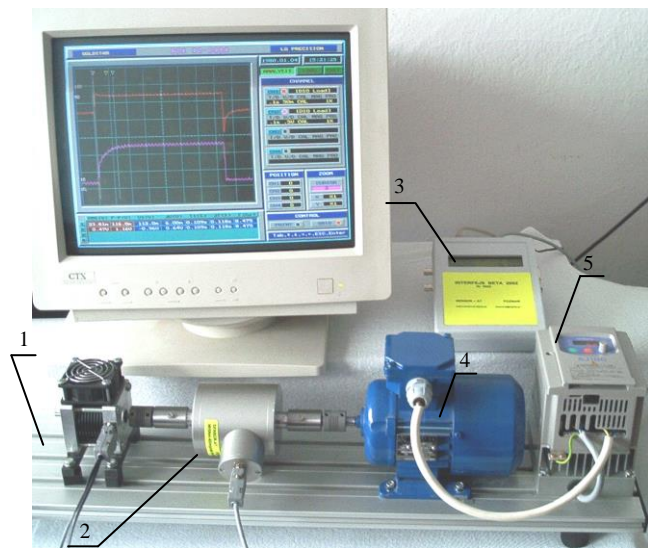


Fig. 11. Test bench for the MRF brake: brake (1), interface BETA (2), torque sensor Mt5Nm (3), induction motor (4), inverter (5)

In order to determine the control characteristics of the brake, the relationship between the braking torque and the exciting current at a constant rotational speed was tested. The measurements were repeated for different values of rotational

speed, in both rotational directions of the rotor. Before each test, the magnetic circuit of the brake was demagnetised. It was found that the direction of rotation does not have any influence on the torque value. The control characteristics for both fluids are shown in Fig. 15. The total braking torque for the current in the exciting coil $I = 0$ and the demagnetised magnetic circuit of the brake is equal to the sum of the torque T_{fr} associated with friction in the seals and bearings and torque $T_c(I, \omega) = T_c(0, \omega)$. The component T_{fr} has been measured for the brake without magnetorheological fluid. The total torque is higher for MRF 132LD because of its higher viscosity (Fig. 1). Higher torque was achieved for this fluid for identical values of the exciting current.

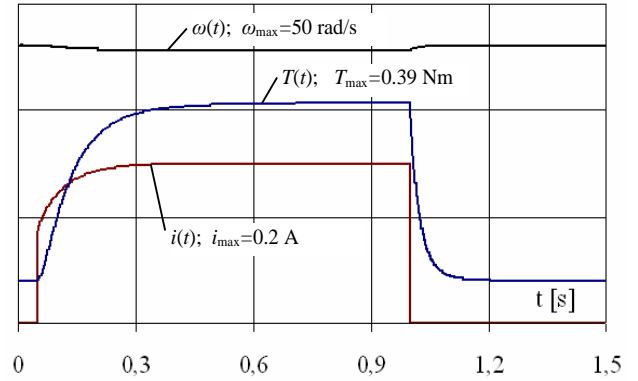


Fig. 12. Calculated torque-time $T(t)$, current-time $i(t)$, and velocity-time $\omega(t)$ characteristics for the length of gap $g = 0.6$ mm

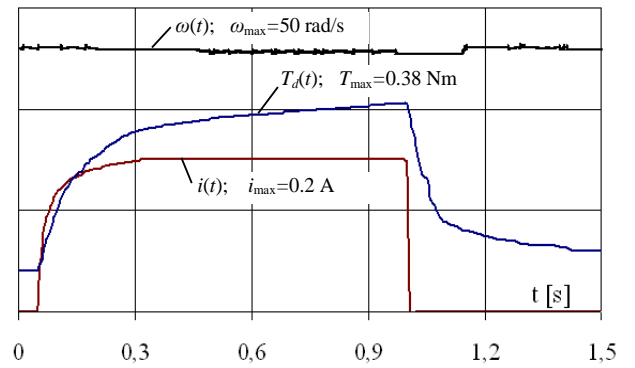


Fig. 13. Measured torque-time $T_d(t)$, current-time $i(t)$, and velocity-time $\omega(t)$ characteristics, $g = 0.6$ mm

Fig. 15 shows also characteristics $T(I)$ calculated by means of the elaborated computer program for the analysis of coupled phenomena in the brake. Good agreement between calculations and measurements has been achieved.

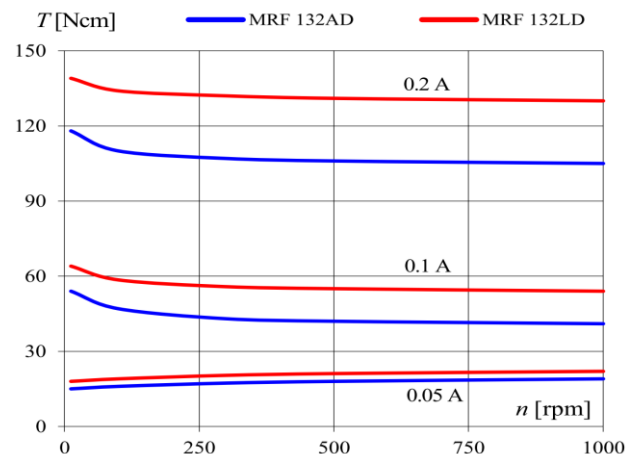


Fig. 14. Mechanical characteristics at constant current values in the excitation winding of the brake, $g = 0.1$ mm

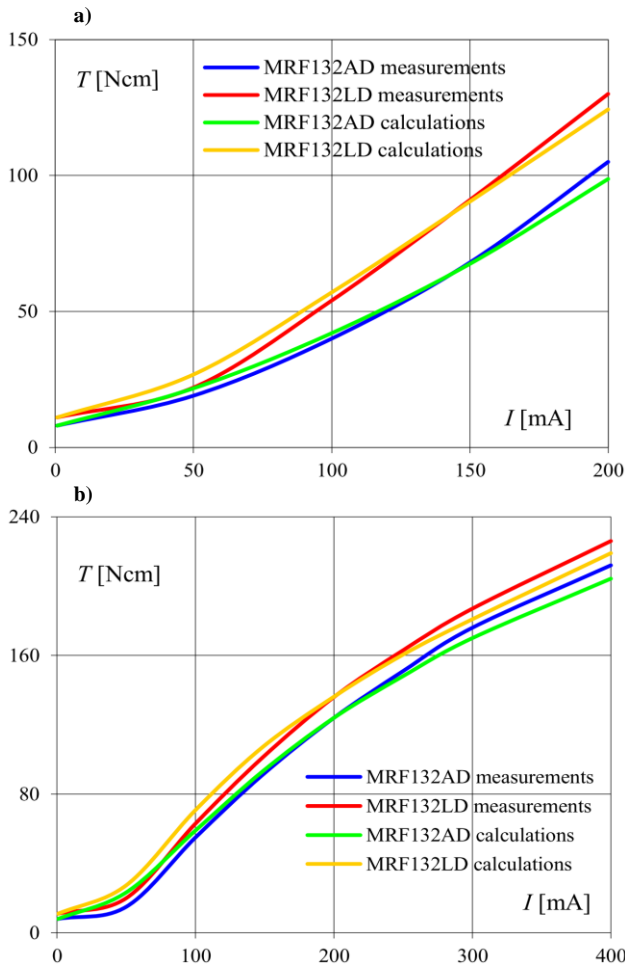


Fig. 15. Relationships between the braking torque and the current in the excitation winding for two different MR fluids at constant rotational speed (a) 1000 rpm (b) 12 rpm; $g = 0.1 \text{ mm}$

The considered disk shape MRF clutch presented in Fig. 4 has been modelled using mesh with about 90 000 triangular elements – see Fig. 16. First the steady state control characteristics of clutching torque T_c vs. winding current I_s have been calculated. To prove model accuracy, the prototype of the clutch and computer-aided experimental setup have been designed and build. The experimental setup components and the clutch prototype are described in Fig. 17. Measurements as well as simulations have been carried out for the braking operation of the clutch – when output rotor was locked ($\omega_2 = 0$). The comparison of simulated and measured control characteristics is shown in Fig. 18.

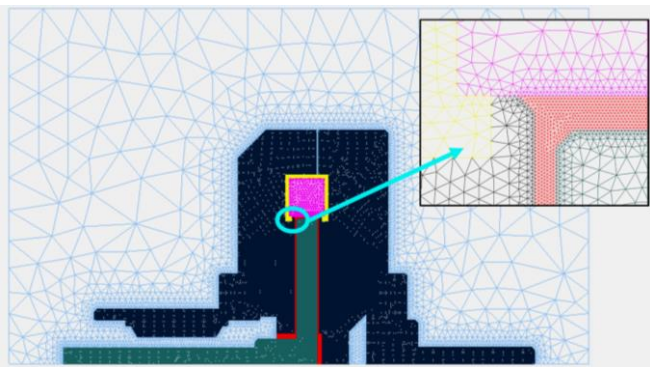


Fig. 16. The mesh of considered clutch (90 000 triangular elements)

Next, the transient state after switching on and off the supply voltage has been investigated. Calculated and measured torque and coil current waveforms are presented in Fig. 19. Exemplary magnetic field distributions and fluid velocity distributions for chosen time instants after switching on the

supply voltage are presented in Fig. 20. The magnetic flux density and fluid velocity plots for chosen time instants after switching off the supply voltage are shown in Fig. 21. It can be observed that the eddy currents induced in massive conducting elements of the considered clutch have a significant impact on the reaction time.

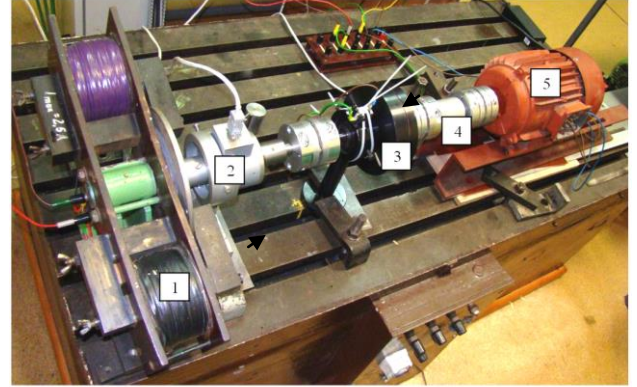


Fig. 17. Experimental setup of disk shape MRF clutch: (1) electromagnetic break, (2) torque sensor, (3) MRF clutch, (4) torque sensor, (5) drive motor

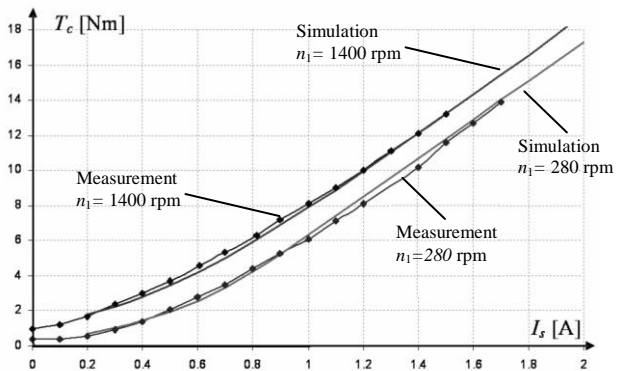


Fig. 18. Control characteristics of clutching torque (T_c) vs. winding current (I_s) for different speeds of the driving motor

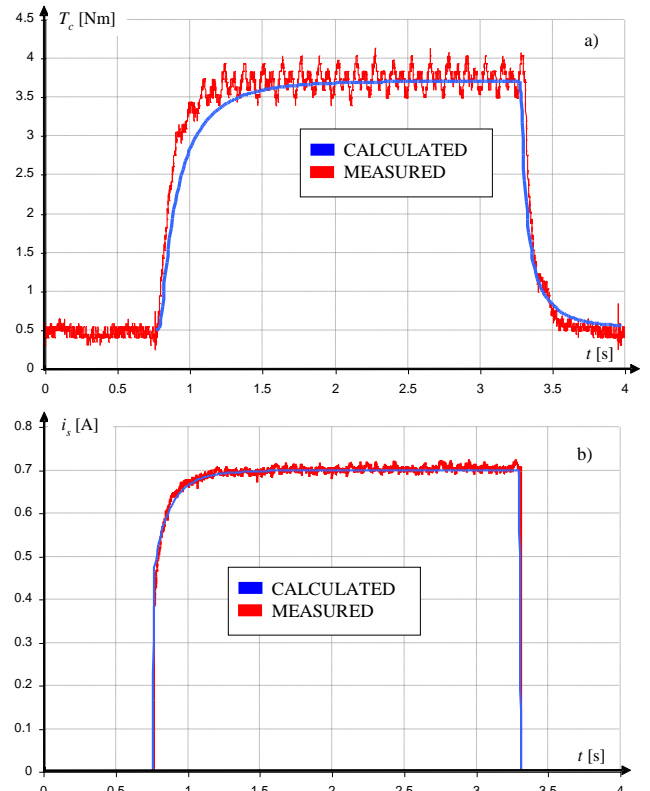


Fig. 19. The calculated and measured a) clutching torque T_c and b) coil current i_s waveforms, after switching on and off the supply voltage

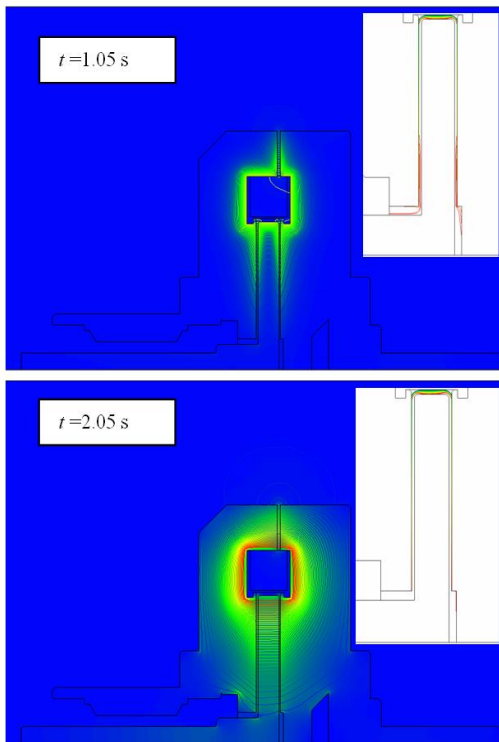


Fig. 20. Magnetic flux lines distributions and fluid velocity distributions for chosen time instants in disk shape MR clutch after switching on the supply voltage



Fig. 21. Magnetic flux lines distributions and fluid velocity distributions for chosen time instants in disk shape MR clutch after switching off the supply voltage

VII. CONCLUSIONS

In the paper, a field model of coupled phenomena in electromechanical transducers with MR fluid was presented. An algorithm for solving the equations of this model was suggested. On the basis of this algorithm, a computer program was developed. The program proved to be useful in simulating transients and steady states of a magnetorheological brake and clutch. In the analysis, the non-linear properties of materials,

the eddy currents induced in solid elements, flows of the fluid, and the rotor movement were considered. The influence of the temperature on electrical, magnetic, and rheological properties of the materials has been taken into account. Good concordance between the calculations and measurements was achieved. The presented model of coupled phenomena and the elaborated calculation software enable a more detailed analysis of the phenomena occurring in magnetorheological transducers than classical analytical models. The approach presented in this paper is very useful in the design process of devices in which magnetorheological fluids are used as a working medium.

VIII. REFERENCES

- [1] Ahmadvkhanlou F., Design, "Modeling and Control of Single and Two Degree of Freedom Magnetorheological Fluid-based Haptic Systems for Telerobotic Surgery", *Journal of Intelligent Material Systems and Structures*, 2009, Vol. 20, No. 10, pp. 1171-1186.
- [2] Baranski M., Demenko A., Lyskawinski W., Szelag W., "Finite element analysis of transient electromagnetic-thermal phenomena in a squirrel cage motor" *COMPEL*, 2011, 30, (3), pp. 832 – 840.
- [3] Baranski. M., Szelag W., "Finite element analysis of transient electromagnetic-thermal phenomena in a squirrel cage motor working at cryogenic temperature", *IET Science Measurement and Technology*, 2012, Vol. 6, Issue 5, pp. 357-363.
- [4] Besbes M., Ren Z., Razek A., "Finite element analysis of magneto-mechanical coupled phenomena in magnetostrictive materials", *IEEE Transactions on Magnetics*, 1996, Vol. 32 No. 3, pp. 1058-1061.
- [5] Bird R.B., Stewart W.E., Lightfoot E.N., *Transport phenomena*, John Wiley & Sons, New, 1960.
- [6] Carlson J.D., Jolly M.R., "MR Fluid, foam and elastomer devices", *Mechatronics*, 2000, 10, pp. 555-569.
- [7] Carlson J.D., Catanizarite D.M., Clair K.A., "Commercial magnetorheological fluid device". *Proc. of 5th Int. Conf. On ER Fluids, MR Suspensions and Associated Technology*, Singapore 1996, pp. 20-28.
- [8] Chaboudez C., Clain S., Glardon R., Rappaz J., Swierkosz M. Touzani R., "Numerical Modelling of Induction Heating of Long Workpieces", *IEEE Transactions on magnetics*, 1994, Vol. 30, No. 6, pp. 5028-5037.
- [9] Driesen J., *Coupled electromagnetic-thermal problems in electrical energy transducers*, Katholieke Universiteit Leuven, Leuven 2000.
- [10] Driesen J., Belmans R.J.M., Hameyer K., "Methodologies for Coupled Transient Electromagnetic-Thermal Finite-Element Modeling of Electrical Energy Transducers", *IEEE Transactions on Industry Applications*, 2002, 38, (5), pp. 1244-1250.
- [11] Driesen J., Hameyer K., "Newton and quasi-Newton algorithms for non-linear electromagnetic-thermal coupled problems", *COMPEL*, 2002, 21, (1), pp. 116-125.
- [12] Demenko A., "Movement simulation in finite element analysis of electric machine dynamics", *IEEE Transactions on Magnetics*, 1996, 32, (3), pp. 1553-1556.
- [13] Demenko A., "Time stepping FE analysis of electric motor drives with semiconductor converter", *IEEE Transactions on Magnetics*, 1994, Vol. 30 No. 5, pp. 3264-3267.
- [14] Hammand K.J., "The effect of hydrodynamic conditions on heat transfer in a complex viscoplastic flow field", *International Journal of Heat and Mass Transfer*, 2000, No. 43, pp. 945-962.

- [15] Jedryczka C., "FE analysis of electromagnetic field coupled with fluid dynamics in an MR clutch", *COMPEL*, 2007, Vol. 26, No. 4, pp.1028 – 1036.
- [16] Jedryczka C., Sujka P., Szlag W., "The influence of magnetic hysteresis on magnetorheological fluid clutch operation", *COMPEL*, Vol. 28, No. 3, 2009, pp. 711-721.
- [17] Jolly M.R., Bender J.W., Carlson J.D., "Properties and applications of commercial magnetorheological fluids", *Journal of Intelligent Material Systems and Structures*, 1999, Vol. 10, No. 1, pp. 5-13.
- [18] Nouar C., Frigaard I.A., "Nonlinear stability of Poiseuille flow of Bingham fluid: theoretical results and comparison with phenomenological criteria", *Journal Non-Newtonian Fluid Mechanics*, 2001, No. 100, pp. 127-149.
- [19] Piriou F., Razek A., "A model for coupled magnetic-electric circuits in electric machines with skewed slots", *IEEE Transactions on Magnetics*, 1990, 26, (2), pp. 1096-1100.
- [20] Rappaz M., Bellem M., Deville M., *Numerical Modeling in Materials Science and Engineering*, Springer, Berlin, 2003.
- [21] Rosensweig R.E., *Ferrohydrodynamics*, Cambridge University Press, 1985.
- [22] Szlag W., "Finite element analysis of coupled magnetorheological fluid devices", *COMPEL*, 2004, Vol. 23, No. 3, pp. 813-824.
- [23] Szlag W., Sujka P., Walendowski R., "Field-circuit transient analysis of a magnetorheological fluid brake", 2004, Vol. 23, No. 4, pp. 986-992.
- [24] Szlag W., "Simulation of coupled phenomena in magnetorheological electromechanical transducers". *Electromotion*, 2002, Vol. 9, No. 4, pp. 181-186.
- [25] Szlag W., "Analysis of coupled phenomena in MR fluid damper", *Archives of Electrical Engineering*, 2007, Vol. LVI, No. 2, pp. 139-148.
- [26] Szlag W., Jedryczka C., Wojciechowski R., Nowak M., "Analysis of magnetic field and temperature influence on shear stresses of magnetorheological fluid" (in Polish), *Electrical Review*, 2009, nr 6, pp. 95-97.
- [27] Szlag W., *Electromagnetic transducers with magnetorheological fluid* (in Polish), Wydawnictwo Politechniki Poznańskiej, 2010.
- [28] Verardi S.L., Cardoso J.R., "A solution of two-dimensional magnetohydrodynamic flow using the finite element method", *IEEE Transactions on Magnetics*, 1998, Vol. 34 No. 5, pp. 3134-3137.
- [29] www.lord.com, information materials.
- [30] www.ferrotec-europe.de, information materials.
- [31] Zienkiewicz O.C., Taylor R.L., Nithiarasu P., *Finite element method for fluid dynamics*, Elsevier, Amsterdam 2005.

AUTHORS' NAMES AND AFFILIATION

Szlag Wojciech
 Poznan University of Technology
 Institute of Electrical Engineering and Electronics
 ul. Piotrowo 3A, 60-965 Poznan, Poland
 Tel: 48 61 665 2116
 E-mail wojciech.szlag@put.poznan.pl

Cezary Jedryczka
 Poznan University of Technology
 Institute of Electrical Engineering and Electronics
 ul. Piotrowo 3A, 60-965 Poznan, Poland
 Tel: 48 61 647 5803
 E-mail cezary.jedryczka@put.poznan.pl